

# 1

## The $sp^2$ Nanocarbons: Prototypes for Nanoscience and Nanotechnology

This chapter presents the reasons why we focus on nanostructured carbon materials as a model materials system for studying Raman spectroscopy and its applications to condensed matter, materials physics and other related science fields. In short, the answer for “why carbon” and “why nano” is the combination of simplicity and richness [1, 2], making possible an unprecedented and accurate exploitation of both the basic fundamentals that link the broad field of condensed matter and materials physics to the applications of Raman spectroscopy, which provides a highly sensitive and versatile probe of the nano-world.

### 1.1

#### Definition of $sp^2$ Nanocarbon Systems

The concept of  $sp^2$  hybridization, where hybridization means the mixing of valence electronic states, is presented here. Carbon has six electrons, two are in  $1s$  states, and four are valence electrons, occupying the  $2s$  and  $2p$  orbitals. The  $1s$  orbitals at around  $E = -285$  eV are occupied by two electrons and the  $1s$  electrons are called core electrons. These core electrons are strongly bound to the nucleus and do not participate in atomic bonding. Thus, they have a small influence on the physical properties of carbon-based materials, and mostly serve as sources for dielectric screening of the outer shell electrons. The second shell  $n = 2$  is more flexible. The energy difference between the  $2s$  and  $2p$  orbitals is less than the energy gain through C–C binding. For this reason, when carbon atoms bind to each other, their  $2s$  and  $2p$  orbitals can mix with one another in  $sp^n$  ( $n = 1, 2, 3$ ) hybridized orbitals. To form the diamond structure, the orbitals for one  $2s$  and three  $2p$  electrons mix, forming four  $sp^3$  orbitals, binding each carbon atom to four carbon neighbors at the vertices of a regular tetrahedron. In contrast, in the  $sp^2$  configuration, the  $2s$  and two  $2p$  orbitals mix to form three in-plane covalent bonds (see Figure 1.1). Here, each carbon atom has three nearest neighbors, forming the hexagonal planar network of graphene. Finally, the  $sp$  hybridization, mixing the orbitals of only one  $2s$  and one  $2p$  electron is also possible, and gives rise to linear chains of carbon atoms, the basis for polyene, the filling of the core of certain nanotubes [3], and providing a step in the coalescence of adjacent nanotubes [4].

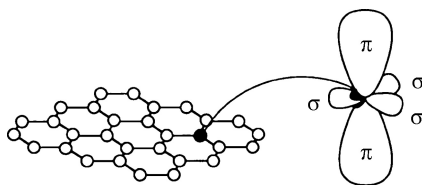


**Figure 1.1** The carbon atomic  $\sigma$  and  $\pi$  orbitals in the  $sp^2$  honeycomb lattice [5].

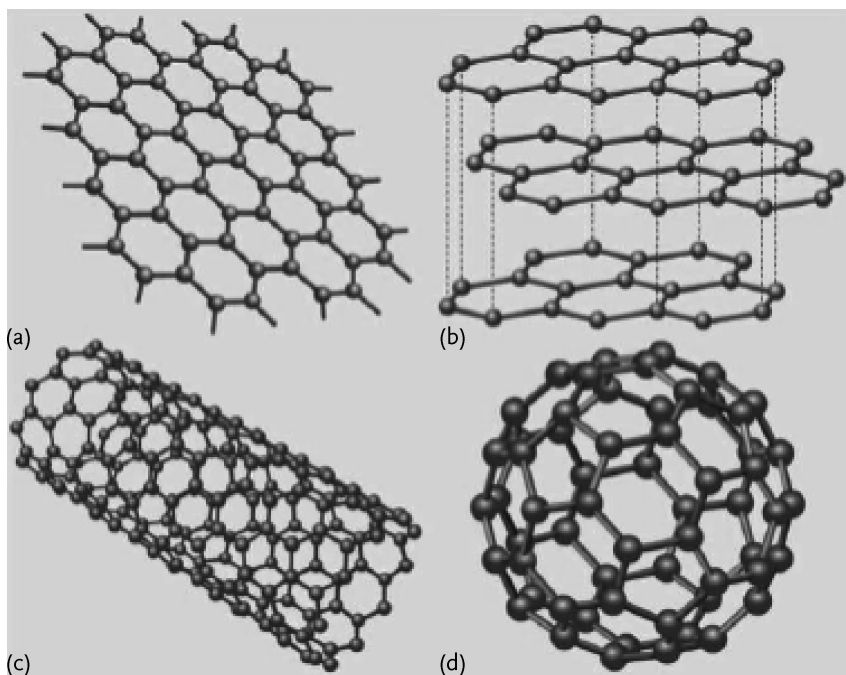


**Figure 1.2** Examples of  $sp^2$  carbon materials, including (a) single-layer graphene, (b) triple-layer graphene, (c) a single-wall carbon nanotube, and (d) a  $C_{60}$  fullerene, which includes 12 pentagons and 20 hexagons in its structure [7, 8].

Having defined the  $sp^2$  hybridization, we now define nanocarbons. The nanocarbons discussed in this book are structures with sizes between the molecular and the macroscopic. The Technical Committee (TC-229) for nanotechnologies standardization of the International Organization for Standardization (ISO) defines nanotechnology as “the application of scientific knowledge to control and utilize matter at the nanoscale, where size-related properties and phenomena can emerge (the nanoscale is the size range from approximately 1 nm to 100 nm).”

The ideal concept of  $sp^2$  nanocarbons starts with the single graphene sheet (see Figure 1.2a), the planar honeycomb lattice of  $sp^2$  hybridized carbon atoms, which is denoted by 1-LG. Although this system can be large (ideally infinite) in the plane, it is only one atom thick, thus representing a two-dimensional  $sp^2$  nanocarbon.

By stacking two graphene sheets, a so-called bilayer graphene (2-LG) is obtained. Three sheets gives three-layer graphene (3-LG), as shown in Figure 1.2b, and many graphene layers on top of each other yield graphite. A narrow strip of graphene (below 100 nm wide) is called a graphene nanoribbon. Rolling-up this narrow strip of graphene in a seamless way into a cylinder forms what is called a single-wall carbon nanotube (SWNT, see Figure 1.2c). Conceptually nanoribbons and nanotubes can be infinitely long, thus representing one-dimensional systems. Add one-, two-layer concentric cylinders and we get double-, triple-wall carbon nanotubes. Many rolled-up cylinders would make a multi-wall carbon nanotube (MWNT). A piece of graphite with small lateral dimensions (a few hundred nanometers and smaller) is called nanographite, which represents a zero-dimensional system. Finally, the “buckyball” (or fullerene) is among the smallest  $sp^2$ - $sp^3$ -like nanocarbon structure (see Figure 1.2d, the most common  $C_{60}$  fullerene) having revolutionized the field of molecular structures. The fullerenes have special properties and can be considered as another class of materials, which are discussed in detail in [6]. As we see, this very flexible  $sp^2$  carbon system gives rise to many different materials with different interesting physics-chemistry related properties that can be studied in depth. And besides its scientific richness, these  $sp^2$  nanocarbons also play a very important role in applications, as discussed in Section 1.2.

## 1.2

### Short Survey from Discovery to Applications

The ideal concept of the different  $sp^2$  nanocarbons starting from graphene, as described above, is didactic, but historically these materials came to human knowledge in the opposite order. Three-dimensional (3D) graphite is one of the longest-known forms of pure carbon, being found on the surface of the earth as a mineral, and formed by graphene planes arranged in an ABAB Bernal stacking sequence [2].<sup>1)</sup> Of all materials, graphite has the highest melting point (4200 K), the highest thermal conductivity (3000 W/mK), and a high room temperature electron mobility (30 000  $\text{cm}^2/\text{Vs}$ ) [9]. Synthetic 3D graphite was made for the first time in 1960 by Arthur Moore [10–15] and was called highly oriented pyrolytic graphite (HOPG). Graphite and its related carbon fibers [16–18] have been used commercially for decades [19]. Their applications range from use as conductive fillers and mechanical structural reinforcements in composites (e. g., in the aerospace industry) to their use as electrode materials exploiting their resiliency (e. g., in lithium ion battery applications) (see Table 1.1) [19, 20].

In 1985 a unique discovery in another  $sp^2$  carbon system took place: the observation of the  $C_{60}$  fullerene molecule [21], the first isolated carbon nanosystem. The fullerenes stimulated and motivated a large scientific community from the time of their discovery up to the end of the century [6], but fullerene-based applications

1) ABAB Bernal stacking is the stacking order of graphene layers as shown in Figure 1.2b. One type of carbon atom (A) aligns in the direction perpendicular to the graphene layer, while the other type (B) aligns in every other layer.

**Table 1.1** Some of the main applications of traditional graphite-based materials including carbon fibers [19].

Traditional graphite materials	Commercial applications
Graphite and graphite-based products	Materials-processing applications such as furnaces/crucibles, large electrodes in metallurgical processes, electrical and electronic devices such as electric brushes, membrane switches, variable resistors, etc., electrochemical applications for electrode materials in primary and secondary batteries, separators for fuel cells, nuclear fission reactors, bearings and seals (mechanical) and dispersions such as inks. (Estimated market in 2008: 13 billion USD)
Carbon-fiber-based products	Carbon-fiber composites Aerospace (70%), sporting goods (18%), industrial equipment (7%), marine (2%), miscellaneous (3%) (Total market in 2008: ~ 1 billion USD)
Carbon-carbon composites	High-temperature structural materials, Aerospace applications, such as missile nose tips, re-entry heat shields, etc., Brake-disc applications (lightweight, high thermal conductivity, stability), Rotating shafts, pistons, bearings (low coefficient of friction), Biomedical implants such as bone plates (biocompatibility) (Estimated market in 2008: 202 million USD).

remain sparse to date. Carbon nanotubes arrived on the scene following the footsteps of the emergence of the  $C_{60}$  fullerene molecule, and they have evolved into one of the most intensively studied materials, now being held responsible for co-triggering the nanotechnology revolution.

The big rush into carbon nanotube science started immediately after the observation of multi-wall carbon nanotubes (MWNTs) on the cathode of a carbon arc system used to produce fullerenes [27], even though they were identified in the core structure of vapor grown carbon fibers as very small carbon fibers in the 1970s [28–30] and even earlier in the 1950s in the Russian literature [23] (see Figure 1.3). However, single-wall carbon nanotubes (SWNTs), the most widely studied carbon nanostructure, were first synthesized intentionally in 1993 [25, 26]. The interest in

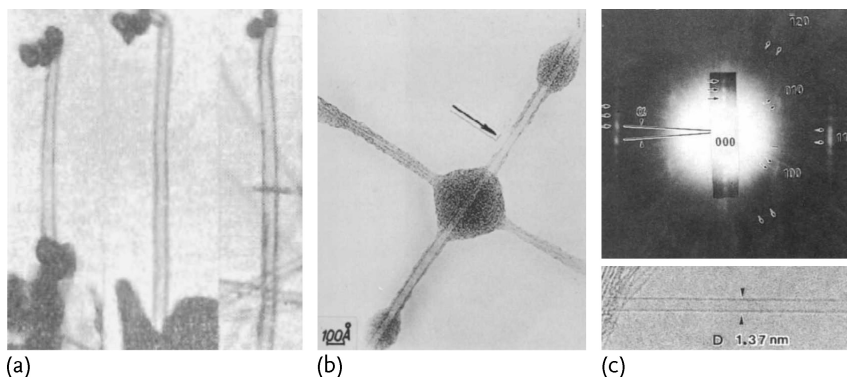


**Figure 1.3** The transmission electron microscopy images of carbon nanotubes [22]. The early reported observations (a) in 1952 [23] and (b) in 1976 [24]. In (c) the observation of single-walled carbon nanotubes that launched the field in 1993 [25] together with [26].

the fundamental properties of carbon nanotubes and in their exploitation through a wide range of applications is due to their unique structural, chemical, mechanical, thermal, optical, optoelectronic and electronic properties [20, 31, 32]. The growth of a single SWNT at a specific location and pointing in a given direction, and the growth of a huge amount of millimeter-long tubes with nearly 100% purity have been achieved [33]. Substantial success with the separation of nanotubes by their  $(n, m)$  structural indices, metallicity (semiconducting and metallic) and by length has been achieved by different methods, as summarized in [33], and advances have been made with doping nanotubes for the modification of their properties, as summarized in [34]. Studies on nanotube mechanical properties [35, 36], optical properties [37–43], magnetic properties [44], optoelectronics [45, 46], transport properties [47] and electrochemistry [48, 49] have exploded, revealing many rich and complex fundamental excitonic and other collective phenomena. Quantum transport phenomena, including quantum information, spintronics and superconducting effects have also been explored [47]. After a decade and a half of intense activity in carbon nanotube research, more and more attention is now focusing on the practical applications of the many unique and special properties of carbon nanotubes (see Table 1.2) [19]. All these advanced topics in the synthesis, structure, properties and applications of carbon nanotubes have been collected in [20].

In the meantime, the study of nanographite was under development as an important model for nano-sized  $\pi$ -electron systems [50]. Its widespread study was launched by the discovery by Novoselov *et al.* [51] of a simple method using Scotch tape to transfer a single atomic layer of  $sp^2$  carbon called graphene (1-LG) from the c-face of graphite to a substrate suitable for the measurement of the electrical and optical properties of monolayer graphene [52]. While the interest in monolayer graphene preparation goes back to the pioneering theoretical work of Wallace in 1947 [53], the Novoselov finding in 2004 led to a renewed interest in what was before considered to be a prototypical system highly valued for theoretical calcu-

**Table 1.2** Applications of nanotubes grouped as present (existing), near-term (to appear in the market within ten years) and long-term (beyond a ten-year horizon), and as categories belonging to large-volume (requiring large amounts of material) and limited-volume (small volume and utilizing the organized nanotube structure) applications [19].

	Large-volume applications	Limited-volume applications (mostly based on engineered nanotube structures)
Present	Battery electrode additives (MWNT) Composites (sporting goods, MWNT) Composites (electrostatic shielding applications, MWNT)	Scanning probe tips (MWNT) Specialized medical appliances (catheters)
Near-term (less than ten years)	Battery and supercapacitor electrodes Multi-functional composites (3D, electrostatic damping) Fuel-cell electrodes (catalyst support) Transparent conducting films Field emission displays/lighting CNT-based inks for printing	Single-tip electron guns Multi-tip array X-ray sources Probe array test systems CNT brush contacts CNT sensor devices Electromechanical memory device Thermal-management systems
Long-term (beyond ten years)	Power transmission cables Structural composites (aerospace and automobile, etc.)	Nanoelectronics (FET, interconnects), flexible electronics CNT-based biosensors CNT in photovoltaic devices CNT filtration/separation membranes, drug-delivery

lations for  $sp^2$  carbons, thereby providing a basis for establishing the structure of graphite, fullerenes, carbon nanotubes and other  $sp^2$  nanocarbons. Surprisingly, this very basic graphene system, which had been studied by researchers over a period of many decades, suddenly appeared with many novel physical properties that were not previously imagined [7, 52]. In one or two years, the rush on graphene science began.

Besides outstanding mechanical and thermal properties (breaking strength  $\sim 40$  N/m, Young's modulus  $\sim 1.0$  TPa, room temperature thermal conductivity  $\sim 5000$  W m $^{-1}$  K $^{-1}$  [54]), the scientific interest in graphene was stimulated by the widespread report of the relativistic (massless) properties of the conduction electrons (and holes) in a single graphene layer less than 1 nm thick, which is responsible for the unusual electrical transport properties in this system (see Figure 1.4) with the state-of-the-art mobility for suspended graphene reaching  $\mu = 200\,000$  cm $^2$ /Vs [55, 56]. Other unusual properties have been predicted and demonstrated experimentally, such as the minimum conductivity and the half-integer quantum Hall effect [57], Klein tunneling [58–64], negative refractive index and Veselago lensing [62], anomalous Andreev reflection at metal-superconductor junc-

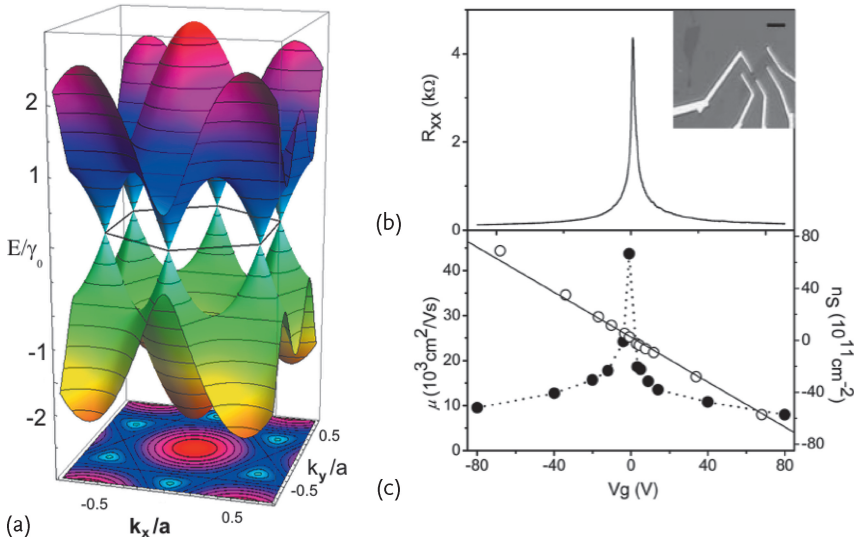


**Figure 1.4** (a) Electronic structure of graphene. The valence and conduction bands touch each other at six points, each called the “Dirac point”. Near these Dirac points, the electron energy ( $E \propto k$ ), giving rise to the Dirac cones, similar to massless particles, like in light cones ( $E = cp$ , where  $c$  is the speed of light). Parts (b) and (c) show transport experiments in a single-layer graphene field effect transistor device. (b) Gate voltage  $V_g$ -dependent in-plane resistance  $R_{xx}$  showing a finite value at the Dirac point. The resistivity

$\rho_{xx}$  can be calculated from the resistance  $R_{xx}$  using the geometry of the device. The inset is an image of a graphene device sitting on a Si:SiO $_2$  substrate. The Si is the bottom gate; five top electrodes formed via e-beam lithography are shown. The scale bar is 5  $\mu\text{m}$ . (c) Mobility  $\mu$  (dotted curve) and carrier density  $n_S$  (solid line) as a function of  $V_g$  (for holes  $V_g < 0$  and for electrons  $V_g > 0$ ). The mobility vs.  $V_g$  diverges but to a finite value at the Dirac point due to the finite resistivity. Adapted from [5].

tions [58, 63–66], anisotropies under antidot lattices [67] or periodic potentials [68], and a metal–insulator transition [69]. Applications as a filler for composite materials, supercapacitors, batteries, interconnects and field emitters have been exploited, although it is still too early to say whether graphene will be able to compete with carbon nanotubes and other materials in the applications world [70].

Finally, graphene can be patterned using high-resolution lithography [71] for the fabrication of nanocircuits with graphene-nanoribbon interconnects. Many groups are now making devices using graphene and also graphene nanoribbons, which have a long length and a small width, and where the ribbon edges play an important role in determining their electronic structure and in exhibiting unusual spin polarization properties [72]. While lithographic techniques have limited resolution for the fabrication of small ribbons ( $< 20$  nm wide), chemical [73] and synthetic [74] methods have been employed successfully, including the unzipping of SWNTs as a route to produce carbon nanoribbons [75, 76].

### 1.3

#### Why $sp^2$ Nanocarbons Are Prototypes for Nanoscience and Nanotechnology

The integrated circuit represents the first human example of nanotechnology, and gave birth to the information age. Together with the nonstop shrinking of electronic circuits, the rapid development of molecular biology and the evolution of chemistry from atoms and molecules into large complexes, such as proteins and quantum dots, have together with other developments launched nanotechnology. It is not possible to clearly envisage the future or the impact of nanotechnology, or even the limit for the potential of nanomaterials, but clearly serious fundamental challenges can already be identified:

- To construct nanoscale building blocks precisely and reproducibly;
- To discover and to control the rules for assembling these nano-objects into complex systems;
- To predict and to probe the emergent properties of these assembled systems.

Emergent properties refer to the complex properties of ensembles of components which exhibit much simpler interactions with their nearest neighbors. These challenges are not only technological, but also conceptual: how to treat a system that is too big to be solved by present day first-principles calculations, and yet too small for using statistical methods? Although these challenges punctuate nanoscience and nanotechnology, the success here will represent a revolution in larger-scale scientific challenges in the fields of emergent phenomena and information technology. Answers to questions like “how do complex phenomena emerge from simple ingredients?” and “how will the information technology revolution be extended?” will probably come from using nanoscience in meeting the challenges of nanotechnology [77].

It is exactly in this context that nanocarbon is expected to play a very important role. On one hand, nature shows that it is possible to manipulate matter and energy the way integrated circuits manipulate electrons, by assembling complex self-replicating carbon-based structures that are able to sustain life. On the other hand, carbon is the upstairs neighbor to silicon in the periodic table, with carbon having more flexible bonding and having unique physical, chemical and biological properties. Nevertheless carbon nanoscience holds promise for a revolution in electronics at some point in the future. Three important factors make  $sp^2$  carbon materials special for facing the nano-challenges listed in the previous paragraph: First is the unusually strong covalent  $sp^2$  bonding between neighboring atoms; second is the extended  $\pi$ -electron clouds coming from the  $p_z$  orbitals; and third is the simplicity of the  $sp^2$  carbon system. We briefly elaborate on these three factors in the following paragraphs.

In the  $sp^2$  configuration, the  $2s$ ,  $p_x$  and  $p_y$  orbitals mix to form three covalent bonds,  $120^\circ$  from each other in the  $x\gamma$  plane (see Figure 1.1). Each carbon atom has three neighbors, forming a hexagonal (honeycomb) network. These  $sp^2$  in-plane bonds are the strongest bonds in nature, comparable to the  $sp^3$  bonds in



diamond, with a measured Young's modulus on the order of 1.0 TPa [54, 78, 79]. This strength is advantageous for  $sp^2$  carbons as a prototype material for the development of nanoscience and nanotechnology, since different interesting nanostructures (sheets, ribbons, tubes, horns, fullerenes, etc.) are stable and strong enough for exposure to many different types of characterization and processing steps.

The  $p_z$  electrons that remain perpendicular to the hexagonal network (see Figure 1.1) form delocalized  $\pi$  electron states which collectively form valence and conduction energy bands. For this reason,  $sp^2$  carbons, which include graphene, graphite, carbon nanotubes, fullerenes and other carbonaceous materials, are also called  $\pi$ -electron materials. The delocalized electronic states in monolayer graphene are highly unusual, because they behave like relativistic Dirac fermions, that is, these states exhibit a massless-like linear energy-momentum relation (like a photon, see Figure 1.4a), and are responsible for unique transport (both thermal and electronic) properties at sufficiently small energy and momentum values [5, 7, 52]. This unusual electronic structure is also responsible for unique optical phenomena, which will be discussed in depth in this book for the case of Raman spectroscopy.

These two physical properties accompany a very important aspect of  $sp^2$  carbons, which is the simplicity of a system formed by only one type of atom in a periodic hexagonal structure. Therefore, different from most materials,  $sp^2$  nanocarbons allow us to easily access their special properties using both experimental and theoretical approaches. Being able to model the structure is crucial for the development of our methodologies and knowledge.

## 1.4

### Raman Spectroscopy Applied to $sp^2$ Nanocarbons

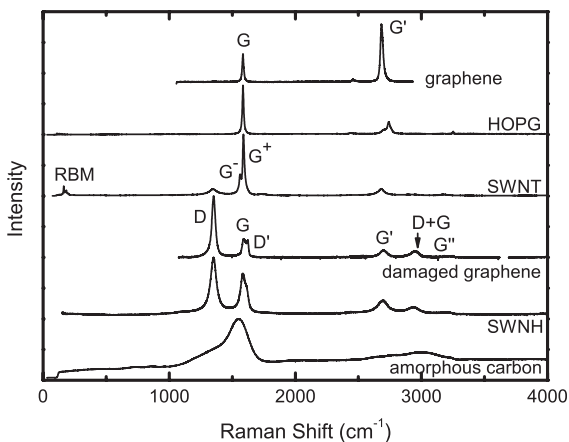
Raman spectroscopy has historically played an important role in the study and characterization of graphitic materials [16, 80], being widely used in the last four decades to characterize pyrolytic graphite, carbon fibers [16], glassy carbon, pitch-based graphitic foams [81, 82], nanographite ribbons [83], fullerenes [6], carbon nanotubes [31, 80], and graphene [84, 85]. For  $sp^2$  nanocarbons, Raman spectroscopy can give information about crystallite size, clustering of the  $sp^2$  phase, the presence of  $sp^3$  hybridization and chemical impurities, mass density, optical energy gap, elastic constants, doping, defects and other crystal disorder, edge structure, strain, number of graphene layers, nanotube diameter, nanotube chirality and metallic vs. semiconductor behavior, as discussed in this book.

Figure 1.5 shows the Raman spectra from different crystalline and disordered  $sp^2$  carbon nanostructures. The first spectrum shown is that for monolayer graphene, the building block of many  $sp^2$  nanocarbons. What is evident from Figure 1.5 is that every different  $sp^2$  carbon in this figure shows a distinct Raman spectrum, which can be used to understand the different properties that accompany each of these different  $sp^2$  carbon structures. For example, 3D highly oriented pyrolytic graphite (labeled HOPG in the figure) shows a distinctly different spectrum from that for

monolayer graphene (1-LG) in Figure 1.5, which in turn is shown to be distinct from the Raman spectra characteristic of the various few layer-graphene materials, for example 2-LG and 3-LG [86].

Figure 1.5 also shows the Raman spectrum for single wall carbon nanotubes (SWNTs). Here we see a variety of features such as the radial breathing mode (RBM) or the splitting of the G-band into  $G^+$  and  $G^-$ -bands that distinguish a SWNT from any other  $sp^2$  carbon nanostructure. Carbon nanotubes are unique materials in many ways, one being their ability to exhibit transport properties that are either metallic (where their valence band and conduction band touch each other at the  $K(K')$  points in the respective graphene Brillouin zone) or semiconducting (where a band gap typically of several hundred meV separates their valence and conduction bands). Nanotubes are also unique in that their Raman spectra differ according to whether the nanotube is semiconducting (as shown in Figure 1.5) or metallic (not shown).

The introduction of disorder breaks the crystal symmetry of graphene and activates certain vibrational modes that would otherwise be silent, such as the D-band and the  $D'$ -band features and their combination  $D + D'$  mode, shown in the spectrum labeled damaged graphene in Figure 1.5. The different types of defects do in fact show their own characteristic Raman spectra, as illustrated in Figure 1.5 by comparing the spectra labeled damaged graphene and SWNH (denoting single-wall carbon nanohorns, another nanostructured form of  $sp^2$  carbon which may include pentagons with a small content of  $sp^3$  bonding [87]). However the topic of distinguishing between the Raman spectra of one and another type of defective graphene remains an area to be explored in detail in the future. When the disorder is so dominant that only near neighbor structural correlations are present (labeled



**Figure 1.5** Raman spectra from several  $sp^2$  nanocarbons. From top to bottom: crystalline monolayer graphene, highly oriented pyrolytic graphite (HOPG), a single-wall carbon nanotube (SWNT) bundle sample, dam-

aged graphene, single-wall carbon nanohorns (SWNH) and hydrogenated amorphous carbon. The most intense Raman peaks are labeled in a few of the spectra [85].

amorphous carbon in the figure), broad first-order and second-order features are seen, with both  $sp^2$  and  $sp^3$  bonding present. Some hydrogen uptake can also occur for such materials to satisfy their dangling bonds [88].

The extremely exciting and rapid development of Raman spectroscopy in  $sp^2$  carbon materials has promoted many advances occurring in this field: graphite is already well-established and commercialized. Carbon nanotubes are by now also mature, after having had an exciting and fast moving research agenda for nearly 20 years. In fact, carbon nanotubes are now ready to make a transition from science to applications, that is at a critical juncture where the laboratory demonstrations of applications need to get translated into product lines. Graphene is younger, but is now attracting many researchers to address the exciting new science hidden in this prototype nanostructure. While the study of the fundamental properties of graphite was essential for understanding the properties of new nanostructured  $sp^2$  carbon forms, further developments of the field are showing how these younger  $sp^2$  carbon nanostructures are revealing many new and unexpected physical phenomena. It is fascinating that Raman spectroscopy has, from the beginning, provided a tool for understanding  $sp^2$  carbon systems. Even after almost a century since the first observation of Raman spectra in carbon-based systems by Sir C. V. Raman himself [89, 90], the Raman spectra from  $sp^2$  carbon materials still puzzle chemists, physicists and material scientists, and these materials offer a challenging system where the worlds of chemistry and physics feed each other.

### Problems

- [1-1] The carbon–carbon distance of graphene (see Figure 1.1) is 1.42 Å. How much area is occupied by a single carbon atom in the graphene plane?
- [1-2] The interlayer distance in multi-layer graphene or graphite (see Figure 1.2b) is 3.35 Å. How much volume is occupied by a single carbon atom in graphite? From this information, estimate the density of graphite in  $\text{g}/\text{cm}^3$ . Compare your estimate with the literature value of  $2.25 \text{ g}/\text{cm}^3$ .
- [1-3] Figure 1.2b shows the AB stacking of graphene layers in forming graphite. Explain how two graphene layers are stacked in the AB stacking sequence.
- [1-4] There are several ways to stack graphene layers. When we put a third layer on the two AB-stacked graphene layers, there are two possible ways of doing this stacking, which we call ABAB and ABC stacking. Show a graphic picture of both ABAB and ABC stacking and explain your answer in words, including the relation between the location of carbon atoms in each relevant plane.
- [1-5]  $\text{C}_{60}$  molecules form face-centered cubic (fcc) structures. The density of the  $\text{C}_{60}$  crystal is  $1.72 \text{ g}/\text{cm}^3$ . From this value, estimate the  $\text{C}_{60}$ – $\text{C}_{60}$  distance and the fcc lattice constants.

- [1-6] Each carbon atom in a  $C_{60}$  molecule has one pentagonal and two hexagonal rings. Calculate the dihedral angles (a) between the two hexagonal rings and (b) between the hexagonal ring and the pentagonal ring.
- [1-7] Diamond crystallizes in a cubic diamond structure with four ( $sp^3$ ) chemical bonds. All bond angles for any pair of chemical bonds are identical. Calculate the bond angle between two chemical bonds by using an analytical solution and also give the numerical value in degrees. The C–C distance in diamond is 1.544 Å. Estimate the cube edge length and density in  $g/cm^3$ .
- [1-8] In spectroscopy, a wave vector is defined by  $1/\lambda$  (where  $\lambda$  is the wavelength) while in solid state physics, the definition of a wave vector is  $2\pi/\lambda$ . Show that a 1 eV photon corresponds to  $8065\text{ cm}^{-1}$  (wavenumbers). In Raman spectroscopy, the difference between the wave vectors for the incident and scattered light is called the Raman shift whose units are generally given in  $\text{cm}^{-1}$ .
- [1-9] Raman spectroscopy involves the inelastic light scattering process. Part of the energy of the incident light is lost or gained, respectively, in materials in which some elemental excitation such as an atomic vibration (phonon) absorbs or releases the energy from or to the light. We call these two Raman processes Stokes and anti-Stokes processes, respectively. When light with the wavelength 632.8 nm is incident on the sample and loses energy by creating a phonon with an energy of 0.2 eV, what is the scattered wavelength? Also give the scattered wavelength for the anti-Stokes Raman signal.
- [1-10] Consider the optical electric field of the incident light with an angular frequency  $\omega_0 = 2\pi\nu_0$  and amplitude  $E_0$ ,

$$E = E_0 \cos \omega_0 t .$$

Then the dipole moment  $P$  of a diatomic molecule is proportional to  $E$  such that  $P = \alpha E$ , in which  $\alpha$  is called the polarizability. When the molecule is vibrating with a frequency  $\omega$ , then  $\alpha$  is also vibrating with the frequency  $\omega$ ,

$$\alpha = \alpha_0 + \alpha_1 \cos \omega t .$$

When substituting  $\alpha$  into the formula  $P = \alpha E$ , show that there are three different frequencies for the scattered light (or  $P$ ),  $\omega_0$  (elastic, Rayleigh scattering) and  $\omega_0 \pm \omega$  (inelastic, Stokes (–) and anti-Stokes (+) Raman scattering).

- [1-11] Let us consider a resonance effect. Here we consider a particle with a mass  $m$  which is connected to a system by a spring with spring constant  $K$ . When we apply an oscillatory force  $f \exp(i\omega t)$ , the equation of motion for the amplitude  $u$  of the vibration is

$$m\ddot{u} + Ku = f \exp(i\omega t) .$$

Solve this differential equation and plot  $u$  after a sufficiently long time as a function of  $\omega$ . Show that a singularity occurs when  $\omega = \omega_0 \equiv \sqrt{K/m}$  and discuss the significance of this singularity.

- [1-12] In a more realistic model than the previous model, we can consider the friction term  $\gamma \dot{u}$  in the vibration

$$m\ddot{u} + \gamma \dot{u} + Ku = f \exp(i\omega t).$$

Plot  $u$  as a function of  $\omega$  for this case. Show that now a singularity no longer occurs. How does  $\gamma$  appear in the plot of  $\omega(u)$ ? Consider the limits of weak damping and strong damping and find what determines the transition between these limits.

